A peer-reviewed version of this preprint was published in PeerJ on 30 August 2019.

Jackson GE, Pavadai E, Gäde G, Andersen NH. 2019. The adipokinetic hormones and their cognate receptor from the desert locust, *Schistocerca gregaria*: solution structure of endogenous peptides and models of their binding to the receptor. PeerJ 7:e7514 https://doi.org/10.7717/peerj.7514

The adipokinetic hormones and their cognate receptor from the desert locust, *Schistocerca gregaria*: solution structure of agonists and model of their binding to the receptor

Graham Ellis Jackson [Corresp., 1], **Elumalai Pavadai** [1], **Gerd Gäde** [2], **Neils Andersen** [3]

[1] Department of Chemistry, University of Cape Town, Cape Town, Western Cape, South Africa

[2] Department of Biological Sciences, University of Cape Town, Cape Town, Western cape, South Africa

[3] Chemistry Department, University of Washington, Seattle, Washington, United States

Corresponding Author: Graham Ellis Jackson
Email address: graham.jackson@uct.ac.za

Background. Neuropeptides exert their activity through binding to G-protein coupled receptors (GPCRs). GPCRs are well-known drug targets in the pharmaceutical industry and are currently discussed as targets to control pest insects. Here we investigate the neuropeptide adipokinetic hormone (AKH) system of the desert locust *Schistocerca gregaria*. The desert locust is known for its high reproduction, and for forming devastating swarms consisting of billions of individual insects. It is also known that *S. gregaria* produces three different AKHs as ligands but has only one AKH receptor. The AKH system is known to be essential for metabolic regulation, which is necessary for reproduction and flight activity.

Methods. Nuclear magnetic resonance techniques (NMR) in a dodecylphosphocholin (DPC) micelle solution were used to determine the structure of the three AKHs. The primary sequence of the *S. gregaria* AKH receptor (AKHR) was used to construct a 3D molecular model. Next, the 3 AKHs were individually docked to the receptor, and dynamic simulation of the whole ligand-receptor complex in a model membrane was performed.

Results. Although the three endogenous AKHs of *S. gregaria* have quite different amino acids sequences and chain length (two octa- and one decapeptide), NMR experiments assigned a turn structure in DPC micelle solution for all. The GPCR-ModSim program identified human kappa opioid receptor (hk-OR) to be the best template after which the *S. gregaria* AKHR was modeled. All three AKHs were found to have the same binding site on this receptor, interact with similar residues of the receptor and have comparable binding constants. Molecular switches were also identified; the movement of the receptor could be visually shown when ligands (AKHs) were docked and the receptor was activated.

Conclusions. The study proposes a model of binding of the three endogenous ligands to the one existing AKH receptor in the desert locust and paves the way to use such a model for the design of peptide analogs and finally, peptide mimetics, in the search for novel species-specific insecticides based on receptor-ligand interaction.

The adipokinetic hormones and their cognate receptor from the desert locust, *Schistocerca gregaria*: solution structure of agonists and model of their binding to the receptor

Graham E. Jackson[1], Elumalai Pavadai[1], Gerd Gäde[2] and Niels H. Andersen[3]

[1] Department of Chemistry, University of Cape Town, Cape Town, South Africa.
[2] Department of Biological Sciences, University of Cape Town, Cape Town, South Africa
[3] Chemistry Department, University of Washington, Seattle, Washington, United States

Corresponding Author:
Graham E. Jackson[1]
Private Bag, Rondebosch, Cape Town, 7701, South Africa.
Email address: graham.jackson@uct.ac.za

Abstract

Background. Neuropeptides exert their activity through binding to G-protein coupled receptors (GPCRs). GPCRs are well-known drug targets in the pharmaceutical industry and are currently discussed as targets to control pest insects. Here we investigate the neuropeptide adipokinetic hormone (AKH) system of the desert locust *Schistocerca gregaria*. The desert locust is known for its high reproduction, and for forming devastating swarms consisting of billions of individual insects. It is also known that *S. gregaria* produces three different AKHs as ligands but has only one AKH receptor. The AKH system is known to be essential for metabolic regulation, which is necessary for reproduction and flight activity.

Methods. Nuclear magnetic resonance techniques (NMR) in a dodecylphosphocholin (DPC) micelle solution were used to determine the structure of the three AKHs. The primary sequence of the *S. gregaria* AKH receptor (AKHR) was used to construct a 3D molecular model. Next, the 3 AKHs were individually docked to the receptor, and dynamic simulation of the whole ligand-receptor complex in a model membrane was performed.

Results. Although the three endogenous AKHs of *S. gregaria* have quite different amino acids sequences and chain length (two octa- and one decapeptide), NMR experiments assigned a turn structure in DPC micelle solution for all. The GPCR-ModSim program identified human kappa opioid receptor (hκ-OR) to be the best template after which the *S. gregaria* AKHR was modelled. All three AKHs were found to have the same binding site on this receptor, interact

with similar residues of the receptor and have comparable binding constants. Molecular switches were also identified; the movement of the receptor could be visually shown when ligands (AKHs) were docked and the receptor was activated.
Conclusions. The study proposes a model of binding of the three endogenous ligands to the one existing AKH receptor in the desert locust and paves the way to use such a model for the design of peptide analogs and finally, peptide mimetics, in the search for novel species-specific insecticides based on receptor-ligand interaction.

Introduction

In 1976 the primary structure of the first metabolic insect neuropeptide was published (Stone et al. 1976). The decapeptide was isolated from the retrocerebral glands called corpora cardiaca (CC) of migratory (*Locusta migratoria*) and desert (*Schistocerca gregaria*) locusts and is functionally paramount in mobilizing lipids, especially during flight episodes and, hence, is denominated adipokinetic hormone (AKH) or code-named today Locmi-AKH-I (for primary structure, see Table 1). In both locust species, a second species-specific AKH octapeptide was found later (Gäde et al. 1986; Siegert et al. 1985) (see Table 1). A third AKH, again an octapeptide, was isolated and functionally characterized from *L. migratoria* (Oudejans et al. 1991) (see Table 1). Genome data mining lead to the discovery of a putative fourth AKH in the migratory locust (Veenstra 2014). The sequence of this octapeptide is identical to an AKH previously cloned from the yellow fever mosquito, Aedes aegypti (Kaufmann et al. 2009) called Aedae-AKH (see Table 1), which is also present in the CC of the alderfly, Sialis lutaria (Gäde et al. 2009). This octapeptide was also identified in the genome of the desert locust (Marchal, Verlinden, Marco, Gäde and Vanden Broeck, unpublished results).
All these peptides are members of the large AKH/red pigment-concentrating hormone (RPCH) family which does not only occur in insects and crustaceans but evolved already in molluscs (Johnson et al. 2014; Li et al. 2016). The AKH gene codes a mRNA that is translated into a pre-propeptide with the following features: a signal peptide is followed immediately by the respective AKH peptide, a glycine amidation site, a dibasic processing site and, C-terminally, another putative peptide of variable length (Gäde & Marco 2013). After cleavage and post-translational modification, the structure of the mature AKH is characterized by a chain length of 8 to 10 amino acids, a pyroglutamate residue (pGlu) at the N-terminus and a carboxyamide at the C-terminus, the amino acids Leu, Ile, Val, Tyr or Phe at position 2, Asn or Thr at position 3, the aromatics Phe or Tyr at position 4, Ser or Thr at position 5, various amino acids at position 6, 7 and 10, the aromatic Trp at position 8 and Gly at position 9 (Gäde 2004; Gäde 2009).
As most insect neuropeptides, AKHs also exert their activity via binding to G protein-coupled receptors (GPCRs). A number of AKH receptors have been cloned and sequenced (Alves-Bezerra et al. 2016; Caers et al. 2012; Hou et al. 2017). GPCRs are well-known drug targets by the pharmaceutical industry and are currently fiercely discussed as targets to control pest insects (Audsley & Down 2015; Verlinden et al. 2014). The AKH system with its metabolic function

has been identified as a putative target as well (Gäde & Goldsworthy 2003). Our first studies characterized the AKH receptor (AKH R) from the desert locust and investigated activation of the cloned receptor in a mammalian cell-based bioluminescence assay by a number of naturally occurring agonists (Marchal et al. 2018).

The available information on ligands and receptor for the *S. gregaria* AKH system gives us the opportunity to study in detail the interaction of the two, and model the putative binding of the ligands to its receptor. This step is necessary to find better agonists, or an antagonist, in order to synthesize new analogues for testing on this system to find adequate and cheap pest insect control substances. Finally, one wants to produce cost-effective peptidomimetics which will bind specifically to the AKH R.

Modelling of binding of members of the AKH/RPCH family to their cognate receptors has been undertaken before: one model has been proposed for an insect, the malaria mosquito, *Anopheles gambiae* (Mugumbate et al. 2013), the other for a crustacean, the water flea *Daphnia pulex* (Jackson et al. 2018). Although the receptors share spatial regions, the binding modes of the two ligands have different orientation (Jackson et al. 2018). In both cases, however, the receptor has only one endogenous octapeptide ligand. In the current study, three agonists (one decapeptide and two octapeptides, see Table 1) are present in *S. gregaria;* these peptides have been found to be active in lipid mobilization (Gäde 1990) (Marco, Verlinden, Marchal, Vanden Broeck and Gäde, unpublished results) and bind to the same receptor (Marchal et al. 2018) (Marchal, Verlinden, Marco, Gäde and Vanden Broeck, unpublished results). The challenge, hence, was to understand the specificity of such a putative model of ligand-receptor interaction.

Materials & Methods

Schgr-AKH-II was synthesized by GL Biochem Ltd (Shanghai, China), Aedae-AKH by Pepmic Co.,Ltd. (Suzhou, China) and Locmi-AKH-I by Peninsula Laboratories (Belmont, California, USA). Purity was checked with HPLC-MS and it was found to be > 95 to 98% pure. The peptides were not sufficiently soluble in water and so solutions were prepared in 30% dimethylsulfoxide (DMSO) and/or in a dodecylphosphocholin (DPC) micelle solution. Typically, 1 mg of sample was dissolved in 0.5 ml of either 20 mM phosphate buffer + 30% DMSO or 10:1 (v/v) H2O:D2O solution which was 150 mM in deuterated DPC-d38 (Cambridge Isotopes, 98.6% d) and buffered at pH 4.5 with 20 mM potassium phosphate buffer and an internal standard of 1% sodium 4,4-dimethyl-4-silapentane-1-sulfonate (DSS). Peptide–peptide interactions were minimized by maintaining a peptide to micelle ratio of 1:3 assuming 50 molecules of DPC per micelle (Jackson et al., 2018).

Nuclear magnetic resonance (NMR) experiments were performed on a Bruker Advance 700 MHz spectrometer or Bruker Advance 600 MHz spectrometer with a prodigy probe. Spectra were recorded with excitation sculpting for water suppression using the dipsi2esgpph pulse sequence (mixing time, 60 ms) for Total Correlation Spectroscopy (TOCSY) (Hwang & Shaka 1995) and noesyesgpph for nuclear Overhauser spectroscopy (NOESY) (Braunschweiler & Ernst

1983) (mixing time, 150 ms). Spectral assignments were based on the method of Wüthrich (Weber et al. 1988; Wüthrich 1986). 13C assignments were based on Heteronuclear Single Quantum Coherence (HSQC) spectra (Sklenar et al. 1993).

Peptide molecular dynamics (MD)

The three AKH peptides were built using Maestro [Schrödinger, Inc., New York, NY, USA] and were energy minimized using a steepest descent algorithm. NMR restrained molecular dynamic simulations in vacuum, water and DPC were performed using GROMACS version 5.1.2 (Van Der Spoel et al. 2005). All simulations were performed using the OPLS-AA all–atom force field with a time step of 2 fs. The LINCS algorithm was used to constraint all bonds. A cut-off of 1.0 nm was used for van der Waals interactions and electrostatic interactions for real space calculations. Vacuum simulations were first done to search conformational space by collecting 100 snapshots of the trajectory during a 10 ns simulation at 600 K. Each conformation was then annealed to 300 K over 40 ps. Cluster analysis of the resulting structures, using the linkage algorithm of GROMACS and a cut-off of 0.1 nm on the backbone atoms, gave a single large cluster. The conformer in the cluster with the lowest energy was used for simulations in water. Using the tip4p water model, a box containing the peptide and ~7000 water molecules was constructed. Following equilibration, molecular dynamics was performed for 10 ns at 300 K under NPT conditions. In total, 200 structures were collected at 50 ps intervals. Cluster analysis was performed as before and the results used in the DPC/water simulations.

For simulations in a water/DPC mixture, the lowest energy structure obtained previously was placed in the center of a 7 nm cubic box filled with ~10 000 SPC water molecules and a 52 DPC molecule micelle as obtained from Tieleman et al.(Tieleman et al. 2000). The micelle was translated so that the center of the micelle was at the bottom edge of the box. This meant that, using periodic boundary conditions, half the micelle was at the bottom of the box and the other half was at the top. The peptide was then placed in the center of the box. Energy minimization was carried out using the steepest descent method to a tolerance of 10 kJ mol-1 or to machine precision. Two stages of system equilibration were performed to solvate the peptide and to achieve a steady state starting temperature, pressure and density. The first stage of equilibration involved performing MD for 100 ps under NVT conditions at 300 K followed in the second stage by a further 1 ns MD under NPT conditions. The final MD simulation was for 10 ns during which 200 snapshots were collected. Cluster analysis was performed in the same manner as before.

Homology modelling

The primary sequence of the target protein, the adipokinetic hormone receptor of S. gregaria, subsequently called Schgr-AKHR, was obtained from the GenBank (GenBank ID: AVG47955.1). Transmembrane (TM) helix predictions (http://bioinf.cs.ucl.ac.uk/psipred/) (Jones 2007; Jones et al. 1994; Nugent & Jones 2009) were computed on-line. The results showed that this sequence has seven TM helices (Figure S1).

GPCR-ModSim Web server (http://gpcr-modsim.org/) (Rodríguez et al. 2012) was used for the template selection and preliminary sequence alignment for building homology models of the Schgr-AKHR. This server accepts an amino acid sequence as input and searches templates by multiple sequence alignments with the query sequence. The GPCR-ModSim identified human kappa opioid receptor (hκ-OR) (PDB ID: 4DJH; Wu et al., 2012) to be the best template. Subsequently, the sequence alignment between Schgr-AKHR and hκ-OR was manually edited to remove gaps in the transmembrane domains without disrupting their conserved regions. Finally, the homology models for the Schgr-AKHR was constructed using Modeler 9v7. This is an automated homology modeling program that performs automated protein homology modeling and loop modeling for the receptor by satisfaction of spatial restraints (Sali 1995). The quality of the selected model was evaluated by a series of test for its internal consistency and reliability such as stereochemical quality, using PROCHECK (Laskowski et al. 1996), and the quality of non-bonded atom interactions using ERRAT (Colovos & Yeates 1993a).

Docking studies

The validated Schgr-AKHR model and the structure of the 3 AKH peptide ligands in a DPC micelle solution, were prepared for docking simulations using *Protein Preparation Wizard* and *LigPrep* of the Schrödinger suite (Schrödinger Inc., New York, NY, USA). Site-directed mutagenesis studies (Kooistra et al. 2013), molecular modelling and structural analyses (Li et al. 2010) suggest that most of the class A GPCRs share a similar binding pocket *c.f.* retinal bound to rhodopsin, carazolol bound to beta-2 adrenergic receptor (Vilar et al. 2011) and Anoga-HrTH bound to AKH receptor of *A. gambiae* (Mugumbate et al. 2011). Thus, the extra-cellular portion of the receptor was used for the docking simulations.

GLIDE docking (Trott & Olson 2010) was used for peptide docking with a grid space of 72 x 72 x 72, which covered all extracellular loops and helices. The receptor grid was generated for peptide ligands and the docking precision was SP-Peptides. This setting automatically increases the number of poses collected.

MD of docked structure

The best poses from the docking studies were used as starting structures for a 2 μs molecular dynamics simulation in a 1-palmitoyl-2-oleoyl-glycero-3-phosphocholine (POPC) membrane. Using the CHARMM-GUI [www.charm-gui.org] the docked complex was placed in a POPC membrane (128 POPC molecules) such that it spanned the membrane. The construct was then converted to an OPLS-AA all–atom force field. Using GROMACS, ~12000 water molecules were added and the charge neutralized by adding Cl^- ions. Several steps of equilibration were used, to get the membrane to pack around the receptor complex. This was followed by 1 μs of NPT simulation at 300 K with Berendsen pressure coupling (Berendsen et al. 1984) and a tau-p of 2.0. The free energy of binding of the final structures, from the dynamic simulations, were calculated using Prime-MM-GBSA (Schrödinger Inc., New York, NY, USA).

Results

Spectral assignment

The chemical shift assignments of the three AKH ligands in DPC are given in Tables 2 – 4. Berjanskii and Wishart (Berjanskii & Wishart 2006) and Tremblay (Tremblay 2010) have shown that by comparing the measured chemical shifts to literature values for a random coil structure, some idea as to the structure and flexibility of the peptide can be obtained. Structuring-induced chemical shift changes (observed shifts minus random coil reference values) were analyzed using the CSDb algorithm available at andersenlab.chem.washington.edu/CSDb/about.php (Eidenschink et al. 2009; Fesinmeyer et al. 2004). Figures 1 a-c show such plots for the three ligands. For Schgr-AKH-II both H^N and H_α are shifted up-field, while for Locmi-AKH-I and Aedae-AKH, only the N^H deviations are up-field. The H_α deviations are small and random. Similar results were found for a number of other deca- and octapeptidic members of the AKH family, i.e. for Declu-CC, Melme-CC and Dappu-RPCH (Jackson et al. 2018). For each of these a β-structuring was found. However, downfield shifts were previously found for the AKH member of the *Anopheles* mosquito, Anoga-HrTH (Mugumbate et al. 2011; Mugumbate et al. 2013).
Using the Random Coil Index tool (Tremblay 2010), the chemical shifts were also used to estimate the model-free order parameter, S2, of the peptides (see Figure 1d). An order parameter of 1 means the peptide is rigid, while an order parameter of 0 means the peptide has no structure. Figure 1d shows that Locmi-AKH-I is very ordered, with a maximum order parameter of 0.9 around proline, whereas the C-terminal has less ordering (S^2 = 0.30). On the other hand, Schgr-AKH-II and Aedae-AKH are much more flexible. The order parameter for these two peptides range from 0.1 to 0.4, which is similar to that of Dappu-RPCH, an AKH peptide member from the crustacean water flea (Jackson et al. 2018).

MD simulation with DPC micelle

Figure 2 shows the solution structures of the 3 AKH ligands in DPC micelle solution. In each case, the molecular dynamics was started with the peptide in water, but they rapidly diffused to interact with the DPC micelle. Depending on the starting orientation of the peptide relative to the micelle, the peptide would make contact with the phospholipid and move away until a stable orientation was established. This is shown in Figure 3 where the peptide/DPC contact area is plotted as a function of time. For Locmi-AKH-I, contact between the DPC and micelle is established during the equilibration period, for Aedae-AKH it is established after 30 ns, while for Schgr-AKH-II, even after 60 ns the peptide is still not permanently attached to the micelle. It is interesting to note that the contact area between Locmi-AKH-I is much higher than that for the other two peptides and Locmi-AKH-I is much more rigid even though it is longer, a decapeptide versus an octapeptide. The interaction between the peptides and the lipid surface, as shown by the contact area, is important as it has been postulated that, before the ligand binds to its receptor, it first binds to the cell membrane surface. Thus, surface binding is an important step in receptor

activation.
Cluster analysis of the trajectory (Fig 2a, b and c) gave a single large cluster for each AKH ligand with a number of smaller clusters. The root conformer and an overlay of each cluster is shown in Figure 2. The predominant conformation of each peptide does have a turn feature but the details differ for each AKH. Locmi-AKH-I (Fig. 2a) has a clear β-turn around its proline residue; Aedae-AKH (Fig. 2b) has a more open structure compared to the other peptides and no marked turn around proline; Schgr-AKH-II (Fig. 2c) is tightly coiled in DPC solution.

Receptor Construct

Use of the GPCR-ModSim server gave the crystal structure of the hκ-OR (PDB ID: 4DJH), with 2.9 Å resolution, as a top template for the Schgr-AKHR. This template has the highest sequence identify compared to other templates as shown in Figure S2. The sequence identity between the Schgr-AKHR and the hκ-OR was 26.33%. The hκ-OR structure belongs to the class A (rhodopsin-like), γ-subfamily of G-protein-coupled receptors (GPCRs) and was selected to build models for the Schgr-AKHR. The template is complexed with the selective antagonist JDTic (Hu et al., 2012). The initial sequence alignment from the GPCR-ModSim was correctly aligned manually with the use of Chimera (Pettersen et al. 2004a; Pettersen et al. 2004b)). The predicted transmembrane helices of Schgr-AKHR and the PDB structural assignments of hκ-OR were also used to confirm the alignment as shown in Figure S1. The sequence analysis shows that the conserved residues of Class A GPCR (hκ-OR) in the seven TM helices (TM1-TM7) are highly conserved within the Schgr-AKHR (conserved residues highlighted by purple coloured boxes in Figure S1), indicating that they may be involved in the function of the Schgr-AKHR such as signalling and ligand binding. Additionally, as in the hκ-OR, disulfide forming cysteine residues (Cys-131 and Cys-210) are conserved in the Schgr-AKHR. The predicted TM helices in the Schgr-AKHR (Figure S3) are consistent with the TM helices of the hκ-OR: there are no gaps or insertions in these regions, signifying that the target sequence is correctly aligned with the template sequence and, hence, can be used for the modelling process.
The homology models of the Schgr-AKHR were built using the *Modeler* 9v7 program. The input parameters of *Modeler* were set to generate 100 models with high structural optimization option. A disulfide bridge, Cys-131–Cys-210, was defined as in the template structure. The best model was selected based on the lowest PDF (molecular probability density function) energies and DOPE score (discrete optimized protein energy) for the docking simulations. The selected models' qualities were subsequently assessed with structural evaluation programs such as PROCHECK and ERRAT. Ramachandran plot analyses of the Schgr-AKHR model from PROCHECK are shown in Figure S4. 100% of residues were either in favoured or in allowed regions, indicating that backbone torsion angles (Phi and Psi) of this model are reliable. In addition, the ERRAT score, so-called overall quality factor, was computed on the Schgr-AKHR model to check the quality of its non-bonded atomic interactions. The normally accepted score range of high-quality model is >50 (Colovos & Yeates 1993b). The ERRAT score for the Schgr-AKHR model was predicted to be 78, showing that the model is within the high-quality range.

All these validation methods demonstrated that the model is reliable and can be used for further studies. The final 3D structure of the Schgr-AKHR model, as shown in Figure S5A, is similar in overall fold with the template protein hκ-OR (Fig. S5B). The superposition of the Schgr-AKHR model with that of the hκ-OR displayed a 2.804 A˚ root mean squared deviation (RMSD) for 1332 atoms pairs. These low RMSDs demonstrate that the overall tertiary structures of the models are similar to the template structure. In addition, the superimpositions indicate that the seven transmembrane helices are highly conserved with hκ-OR. However, there are slight structural variations in the loop regions of the model.

Ligand Docking

LigPrep was used to generate multiple conformers of the three AKH peptides, which were then docked to the Schgr-AKHR. A receptor grid was generated for the extra-cellular half of the GPCR and the peptide docked using SP-Peptide precision. One hundred different poses were collected and scored for each peptide. An overlay of the highest scoring poses gave the same receptor binding site for all three peptides. This binding pocket consisted of a cleft running across the top of the Schgr-AKHR, between helices 2, 6 and 7 and extra-cellular loops 2 and 4 (details shown in Figures 4 – 6). The ligands lay along this cleft. It was found that, while the GLIDE protocol tried to dock many different conformations of the peptide, only those with some turn structure were successful. Many of the docked poses had similar GLIDE scores but different sets of peptide/receptor interactions. During the docking, it was found that the orientation of the peptide within the binding pocket did not change. For this reason, the docking was repeated with the peptide rotated through 180 degrees around the axis of the transmembrane helices i.e., the direction of N-terminus to the C-terminus was reversed. Again, the peptide could be docked successfully, indicating that the binding pocket was quite promiscuous. Although either orientation of the peptide would bind to the receptor, the binding energies of the two orientations differed by some 50 kcal/mol and hence the original orientation (shown below) was chosen for further study.

The docked structure of each AKH peptide with the highest binding energy, was used as the starting structure for molecular dynamics of the complex in a POPC membrane. During the dynamics, the ligands were found to move, and individual side-chains rotate within the binding site making and breaking H-bonds to various residues of the receptor. This was essentially the same as what was found during the GLIDE docking. While the POPC membrane added to the computational cost of the simulation, it was necessary to prevent the receptor, trans-membrane helices, from moving apart. Snapshots of the simulation were transferred to Maestro, where Prime-MM-GBSA was used to estimate the binding energy.

Figure 4a and b shows an overlay of several snapshots of the dynamic simulation of the octapeptide, Schgr-AKH-II, in its receptor binding pocket. As can be seen, the overall conformation of Schgr-AKH-II remains the same (Figure 4c) but the side-chains move within the binding site, forming and breaking intra- and inter-molecular H-bonds. There is also some movement of the receptor during the dynamics. The free energy of binding of the different

snapshots were not significantly different and ranged from -94 to -116 kcal/mol over the 1 μs simulation.

The bound conformation of Schgr-AKH-II is shown in Figure 4c, while Figure 4d is an overlay of bound Schgr-AKH-II and its lowest energy conformation in DPC micelle solution. The agreement of these generated conformers is remarkable, especially considering that the GLIDE – SP protocol generates some 100 different starting conformations for the peptide docking.

Figure 5a shows the bound conformation of Locmi-AKH-I, while Figure 5b is an overlay of this bound conformer and the lowest energy conformer found in DPC micelle solution. The agreement here is not as close as that for Schgr-AKH-II, but the same turn structure is seen.

Figure 5c shows Locmi-AKH-I in the receptor binding pocket, while Figures 5d and e show the details of how Locmi-AKH-I fits into the Schgr-AKHR: the decapeptide stretches across the cleft in the receptor with the central portion of the peptide fitting into the binding pocket, but the two termini pointing outside the binding pocket. Locmi-AKH-I gave the most trouble during the docking stage as poses were frequently rejected. During the molecular dynamics, the terminal amide of this decapeptide was sometimes found to H-bond to a POPC molecule, which is of course not present during the GLIDE docking. The final binding energy for Locmi-AKH-I was -98 kcal/mol.

Figure 6a and b show how Aedae-AKH fits into the binding pocket of the Schgr-AKHR. The arrangement is similar to that of Locmi-AKH-I, except, in this case, the termini do not extend outside the receptor. In the case of Aedae-AKH, ECL4 folds over the top of the binding site, trapping the peptide inside. The conformation of bound Aedae-AKH is shown in Figure 6c, and an overlay with the DPC micelle solution conformation is shown in Figure 6d. Again, these two conformations are very similar, supporting the idea that the peptides are pre-arranged on the cell surface. The binding energy of Aedae-AKH was -88 kcal/mol.

Ligand interaction diagrams for the three ligands are shown in Figure 7, while Table 5 lists the interactions between the ligands and the Schgr-AKHR. From these data, it is clear that all three AKH ligands have very similar interactions with Schgr-AKHR. Both Schgr-AKH-II and Aedae-AKH, H-bond to His169 of the receptor, while W^8 of Locmi-AKH-I π-stacks with this residue. In Locmi-AKH-I, the amide carbonyl, pE^1CO, H-bonds to Lys281, while in Aedae-AKH it is $pE^1O_{\varepsilon 1}$ which H-bonds to Lys281. The terminal residue of both Schr-AKH-II and Locmi-AKH-I H-bond to Lys288.

Analysis of molecular switches

A feature of class A GPCRs is the presence of highly conserved molecular switch motifs. These switches, which play key roles in the stabilization of the receptor in an inactive and active state include a TM3-6 lock, a SPLF switch, a tyrosine toggle and a DRY ionic lock. The breaking of these switches results in movement of the transmembrane helices, which can activate the receptor (Trzaskowski et al. 2012). These switches are the same as those reported for the AKH-R receptor of *Drosphilia melanogaster*, *Tribolium castaneum, A. gambiae* and *Rhodnius prolixus*

(Rasmussen et al. 2015) suggesting that the activation mechanism of Schgr-AKHR may be the same.

The DRY ionic lock between arginine and tyrosine is postulated to open and close during receptor activation. This is shown in Figure 8. In the inactive state, the DRY switch is closed (Figure 8b) but upon ligand binding, TM6 and TM3 twist, opening this switch (Figure 8c).

The TM3-6 lock involves two residues in the binding pocket, Arg^{107} on TM3 and Tyr^{265} on TM6 (Figure 9a). In the inactive state these two residues are far apart, but on ligand activation, they move closer together. Fig 9a also shows, in the active state, Arg^{107} H-bonding with Glu^{190} of ECL4. It was noted before that this loop closes over the binding pocket after ligand binding. In Fig 9a one can also clearly see how TM6 and TM3 move together on the extra-cellular side but move away from each other on the intra-cellular side, upon activation.

The tyrosine toggle switch involves the NPxxY motif on TM7 and Tyr^{213} on TM5 (Fig 9b).

Discussion

As has been found before, insect neuropeptides are flexible in solution but generally have a preferred β-turn conformation (Mercurio et al. 2018; Shen et al. 2018; Zubrzycki 2000). Using CD spectroscopy, Cusinato et al. (Cusinato et al. 1998) proposed a P II extended conformation for the AKH/RPCH peptides, at low temperatures, in aqueous solution. However, they found that the majority of AKH/RPCH peptides adopted a β-turn conformation in the presence of 0.6% SDS. This is what was found in DPC micelle solution by both NMR chemical shift and molecular modelling results for the three peptides Schgr-AKH-II, Aedae-AKH and Locmi-AKH-I in the current study. These peptides are not very soluble in water but are readily soluble in DPC micelle solution, which is a clear indication that they interact with the micelle. Previously, using DOSY NMR spectroscopy, we showed that the crustacean AKH member, Dappu-RPCH, binds to the micelle in DPC solution, and that the micelle consists of ~ 50 DPC molecules (Jackson et al. 2018). This was also shown by the molecular modelling for the 3 locust peptides in the present study. Locmi-AKH-I interacted strongly with the micelle and perhaps this is the reason why this peptide had a much higher order parameter than the other two peptides.

Despite chain length and sequence differences all three peptides were found to bind to the same binding site of the receptor. They all had similar binding constants and interacted with the same receptor residues. This is in agreement with previous results of Marchal et al. (Marchal et al. 2018) where many members of the AKH family activated the Schgr-AKHR in vitro to the same extent and it was concluded that this receptor was quite promiscuous. In the present study, multiple binding poses were found for the peptides in the binding site and this was confirmed by the molecular dynamics in a POPC membrane. Here each peptide was found to move within the binding site, interacting with different residues. This may account for the same receptor being activated naturally by all three peptides. Interestingly, during the molecular dynamics, the receptor itself moved, closing over the binding site and opening up on the intra-cellular side. This motion has been postulated to result in receptor activation, with a G-protein able to bind to the more open receptor. Figure 8a, which is an overlay of the active and inactive receptor,

shows this movement of the helices. Measurements show that Ala-243 on TM6 moves some 6.4 Å on receptor activation. One can also see that ECL6 and ECL4 (Figure 4b) close over the binding site.

It is interesting to compare and contrast the binding of Schgr-AKH-II, Aedae-AKH and Locmi-AKH-I with the binding of a crustacean red pigment-concentrating hormone from *Daphnia pulex*, Dappu-RPCH, to its cognate receptor, Dappu-RPCHR(Jackson et al. 2018). Both receptors have similar binding sites involving TM2, 6 and 7 but Dappu-RPCHR also uses extracellular loops 1, 2 and 3, while Schgr-AKHR involves loops 2 and 4 (and loop 6 in the active receptor). Dappu-RPCH undergoes significant conformational changes upon receptor binding, having a more extended structure in solution but a more pronounced β-turn when bound. On the other hand, Schgr-AKH-II, Aedae-AKH and Locmi-AKH-I, undergo very little conformational change upon receptor binding. This might account for the higher binding constant of these three peptides relative to Dappu-RPCH. The similarity between the AKH/RPCH systems is understandable given the evolution of the AKH/corazonin/ACP/GnRH receptor superfamily and their ligands. (Hauser & Grimmelikhuijzen 2014)

The presented model of Schgr-AKHR can be compared to another class A GPCR, the human gonadotropin releasing hormone receptor, GnRHR (Flanagan & Manilall 2017). This receptor has an exaggerated bend around Pro, in a CWxPY motif found on TM6. In GnRHR, this bend is stabilized by a water mediated H-bond between Cys^{47} on and Tyr^{51} on TM6 of the CWxPY motif and by H-bonding to a residue in TM7. The presented model of Schgr-AKHR also has this CWxPY motif in TM6, which results in a proline kink. In the active receptor, Cys and Tyr residues are correctly oriented for water mediated H-bonding, with a distance of 3.18 Å between them. Also, Trp^{262} of the CWxPY motif was found to H-bond to Asn^{297} of TM7. The functional importance of this motif has been demonstrated by mutations associated with congenital hypogonadotropic hypogonadism (CHH). This rare disorder results from decreased production or secretion of gonadotropin-releasing hormone (GnRH) and/or lack of action of GnRH upon GnRHR. There are some 25 genes identified in this condition, but if the Pro residue is substituted by Arg, there is complete disruption of the receptor function. This shows the importance of this proline kink. On the other hand, when the Cys, of this receptor motif, is mutated to Tyr or Ala, the GnRH ligand does not bind to the receptor (Flanagan & Manilall 2017). Interestingly, in the inactive Schgr-AKHR, there was a H-bond between Trp-CO and Tyr-NH but there was no H-bond between Trp^{262} and Asn^{297}. Upon ligand binding, however, the helices moved in such a way that the one H-bond broke and the other formed. This is similar to the DRY switch described above. Binding similarities between GnRHR and Schgr-AKHR are not unexpected. It is accepted since a few years that GnRH and AKH are peptides belonging to the same superfamily because not only are the ligands structurally closely related but also the cognate receptors (Gäde et al. 2011; Hauser & Grimmelikhuijzen 2014; Roch et al. 2011; Roch et al. 2014).

Conclusions

In this paper, we have shown that the putative receptor, Schgr-AKHR, is a member of the Class A superfamily of G-protein coupled receptors. It has 7 transmembrane helices and the same conserved residues as other AKH receptors. Schgr-AKHR also has a number of molecular switch motifs, which are a feature of class A GPCRs. Our results show that the three endogenous peptides, Schgr-AKH-II, Aedae-AKH and Locmi-AKH-I, all bind to the same receptor binding site and with very similar binding constants. This may be surprising, as the three ligands are very different. However, *L. migratoria and S. gregaria*, have only one AKH receptor so it could be expected. These results also fit previous findings that, in vitro, the AKH receptor of *S. gregaria* is equally well activated by a number of AKH members.

The similarity between the ligand binding of Schgr-AKHR and Dappu-RPCH/Dappu-RPCHR supports the evolutionary development of the AKH/corazonin/ACP/GnRH receptor superfamily. The next step in this study would be to use *in silico* screening to identify suitable antagonists, which could act as next generation insecticides.

References

Alves-Bezerra M, De Paula IF, Medina JM, Silva-Oliveira G, Medeiros JS, Gäde G, and Gondim KC. 2016. Adipokinetic hormone receptor gene identification and its role in triacylglycerol metabolism in the blood-sucking insect *Rhodnius prolixus*. *Insect biochemistry and molecular biology* 69:51-60. https://doi.org/10.1016/j.ibmb.2015.06.013

Audsley N, and Down RE. 2015. G protein coupled receptors as targets for next generation pesticides. *Insect biochemistry and molecular biology* 67:27-37. S0965-1748(15)30030-8 [pii]

Berendsen HJC, Postma JPM, van Gunsteren WF, DiNola A, and Haak JR. 1984. Molecular dynamics with coupling to an external bath. *The Journal of Chemical Physics* 81:3684-3690.

Berjanskii M, and Wishart DS. 2006. NMR: Prediction of protein flexibility. *Nature Protocols* 1:683-688.

Braunschweiler L, and Ernst RR. 1983. Coherence transfer by isotropic mixing - Application to proton correlation spectroscopy. *J Magn Reson* 53:521-528.

Caers J, Peeters L, Janssen T, De Haes W, Gäde G, and Schoofs L. 2012. Structure-activity studies of *Drosophila* adipokinetic hormone (AKH) by a cellular expression system of dipteran AKH receptors. *General and Comparative Endocrinology* 177:332-337. 10.1016/j.ygcen.2012.04.025

Colovos C, and Yeates TO. 1993a. Verification of Protein Structures - Patterns of Nonbonded Atomic Interactions. *Protein Science* 2:1511-1519.

Colovos C, and Yeates TO. 1993b. Verification of protein structures: Patterns of nonbonded atomic interactions. *Protein Science* 2:1511-1519.

Cusinato O, Drake AF, Gäde G, and Goldsworthy GJ. 1998. The molecular conformations of representative arthropod adipokinetic peptides determined by circular dichroism spectroscopy. *Insect biochemistry and molecular biology* 28:43-50. https://doi.org/10.1016/S0965-1748(97)00094-5

Eidenschink L, Kier BL, Huggins KNL, and Andersen NH. 2009. Very short peptides with stable folds: Building on the interrelationship of Trp/Trp, Trp/cation, and Trp/backbone amide interaction geometries. *Proteins: Structure, Function, and Bioinformatics* 75:308-322. 10.1002/prot.22240

Fesinmeyer RM, Hudson FM, and Andersen NH. 2004. Enhanced hairpin stability through loop design: The case of the protein G B1 domain hairpin. *Journal of the American Chemical Society* 126:7238-7243. 10.1021/ja0379520

Flanagan CA, and Manilall A. 2017. Gonadotropin-Releasing Hormone (GnRH) Receptor Structure and GnRH Binding. *Frontiers in Endocrinology* 8:274.

Gäde G. 1990. Structure–function studies on hypertrehalosaemic and adipokinetic hormones: activity of naturally occurring analogues and some N- and C-terminal modified analogues. *Physiological Entomology* 15:299-316. 10.1111/j.1365-3032.1990.tb00518.x

Gäde G. 2004. Regulation of intermediary metabolism and water balance of insects by neuropeptides. Annual Review of Entomology. p 93-113.

Gäde G. 2009. Peptides of the Adipokinetic Hormone/Red Pigment-Concentrating Hormone Family. *Annals of the New York Academy of Sciences* 1163:125-136.

Gäde G, and Goldsworthy GJ. 2003. Insect peptide hormones: a selective review of their physiology and potential application for pest control. *Pest Management Science* 59:1063-1075. 10.1002/ps.755

Gäde G, Goldsworthy GJ, Schaffer MH, Cook JC, and Rinehart KL. 1986. Sequence analyses of adipokinetic hormones II from corpora cardiaca of *Schistocerca nitans*, *Schistocerca gregaria*, and *Locusta migratoria* by fast atom bombardment mass spectrometry. *Biochem Biophys Res Commun* 134:723-730.

Gäde G, and Marco HG. 2013. Chapter 28 - AKH/RPCH Peptides. In: Kastin AJ, ed. *Handbook of Biologically Active Peptides (Second Edition)*. Boston: Academic Press, 185-190.

501 Gäde G, Šimek P, and Marco HG. 2009. The first identified neuropeptide in the insect order
502 Megaloptera: A novel member of the adipokinetic hormone family in the alderfly *Sialis lutaria*.
503 *Peptides* 30:477-482.

504 Gäde G, Šimek P, and Marco HG. 2011. An invertebrate [hydroxyproline]-modified
505 neuropeptide: Further evidence for a close evolutionary relationship between insect adipokinetic
506 hormone and mammalian gonadotropin hormone family. *Biochemical and Biophysical Research*
507 *Communications* 414:592-597. https://doi.org/10.1016/j.bbrc.2011.09.127

508 Hauser F, and Grimmelikhuijzen CJP. 2014. Evolution of the AKH/corazonin/ACP/GnRH
509 receptor superfamily and their ligands in the Protostomia. *General and Comparative*
510 *Endocrinology* 209:35-49. 10.1016/j.ygcen.2014.07.009

511 Hou Q-L, Chen E-H, Jiang H-B, Wei D-D, Gui S-H, Wang J-J, and Smagghe G. 2017.
512 Adipokinetic hormone receptor gene identification and its role in triacylglycerol mobilization
513 and sexual behavior in the oriental fruit fly (*Bactrocera dorsalis*). *Insect biochemistry and*
514 *molecular biology* 90:1-13. https://doi.org/10.1016/j.ibmb.2017.09.006

515 Hwang TL, and Shaka AJ. 1995. Water Suppression That Works. Excitation Sculpting Using
516 Arbitrary Wave-Forms and Pulsed-Field Gradients. *Journal of Magnetic Resonance, Series A*
517 112:275-279. https://doi.org/10.1006/jmra.1995.1047

518 Jackson GE, Pavadai E, Gäde G, Timol Z, and Andersen NH. 2018. Interaction of the red
519 pigment-concentrating hormone of the crustacean *Daphnia pulex*, with its cognate receptor,
520 Dappu-RPCHR: A nuclear magnetic resonance and modeling study. *International Journal of*
521 *Biological Macromolecules* 106:969-978. https://doi.org/10.1016/j.ijbiomac.2017.08.103

522 Johnson JI, Kavanaugh SI, Nguyen C, and Tsai P-S. 2014. Localization and Functional
523 Characterization of a Novel Adipokinetic Hormone in the Mollusk, *Aplysia californica*. *PLOS*
524 *One* 9:e106014. 10.1371/journal.pone.0106014

525 Jones DT. 2007. Improving the accuracy of transmembrane protein topology prediction using
526 evolutionary information. *Bioinformatics* 23:538-544.

527 Jones DT, Taylor WR, and Thorton JM. 1994. A Model Recognition Approach to the Prediction
528 of All-Helical Membrane-Protein Structure and Topology. *Biochemistry* 33:3038-3049.

529 Kaufmann C, Merzendorfer H, and Gäde G. 2009. The adipokinetic hormone system in
530 Culicinae (Diptera: Culicidae): Molecular identification and characterization of two adipokinetic
531 hormone (AKH) precursors from *Aedes aegypti* and *Culex pipiens* and two putative AKH
532 receptor variants from *A. aegypti*. *Insect biochemistry and molecular biology* 39:770-781.

Kooistra AJ, Kuhne S, De Esch IJP, Leurs R, and De Graaf C. 2013. A structural chemogenomics analysis of aminergic GPCRs: Lessons for histamine receptor ligand design. *British Journal of Pharmacology* 170:101-126. 10.1111/bph.12248

Laskowski RA, Rullmann JAC, MacArthur MW, Kaptein R, and Thornton JM. 1996. AQUA and PROCHECK-NMR: Programs for checking the quality of protein structures solved by NMR. *Journal of Biomolecular NMR* 8:477-486.

Li S, Hauser F, Skadborg SK, Nielsen SV, Kirketerp-Møller N, and Grimmelikhuijzen CJP. 2016. Adipokinetic hormones and their G protein-coupled receptors emerged in Lophotrochozoa. *Scientific Reports* 6:32789. 10.1038/srep32789 https://www.nature.com/articles/srep32789 - supplementary-information

Li YY, Hou TJ, and Goddard III WA. 2010. Computational modeling of structure-function of G protein-coupled receptors with applications for drug design. *Current Medicinal Chemistry* 17:1167-1180. 10.2174/092986710790827807

Marchal E, Schellens S, Monjon E, Bruyninckx E, Marco H, Gäde G, Vanden Broeck J, and Verlinden H. 2018. Analysis of Peptide Ligand Specificity of Different Insect Adipokinetic Hormone Receptors. *International Journal of Molecular Science* 19(2) pii E542 doi: 10.3390/ijms19020542.

Mercurio FA, Scaloni A, Caira S, and Leone M. 2018. The antimicrobial peptides casocidins I and II: Solution structural studies in water and different membrane-mimetic environments. *Peptides*. https://doi.org/10.1016/j.peptides.2018.09.004

Mugumbate G, Jackson GE, and van der Spoel D. 2011. Open conformation of adipokinetic hormone receptor from the malaria mosquito facilitates hormone binding. *Peptides* 32:553-559. 10.1016/j.peptides.2010.08.017

Mugumbate G, Jackson GE, van der Spoel D, Koever KE, and Szilagyi L. 2013. *Anopheles gambiae*, Anoga-HrTH hormone, free and bound structure - A nuclear magnetic resonance experiment. *Peptides* 41:94-100. 10.1016/j.peptides.2013.01.008

Nugent T, and Jones DT. 2009. Transmembrane protein topology prediction using support vector machines. *BMC Bioinformatics* 10. 10.1186/1471-2105-10-159

Oudejans RCHM, Kooiman FP, Heerma W, Versluis C, Slotboom AJ, and Beenakkers AMT. 1991. Isolation and structure elucidation of a novel adipokinetic hormone (Lom-AKH-III) from the glandular lobes of the corpus cardiacum of the migratory locust, *Locusta migratoria*. *Eur J Biochem* 195:351-359.

Pettersen EF, Goddard TD, Huang CC, Couch GS, Greenblatt DM, Meng EC, and Ferrin TE. 2004a. UCSF Chimera - A visualization system for exploratory research and analysis. *Journal of Computational Chemistry* 25:1605-1612. 10.1002/jcc.20084

Pettersen EF, Goddard TD, Huang CC, Couch GS, Greenblatt DM, Meng EC, and Ferrin TE. 2004b. UCSF Chimera—a visualization system for exploratory research and analysis. *Journal of Computational Chemistry* 25:1605-1612.

Rasmussen M, Leander M, Ons S, and Nichols R. 2015. Conserved molecular switch interactions in modeled cardioactive RF-NH2 peptide receptors: Ligand binding and activation. *Peptides* 71:259-267. 10.1016/j.peptides.2015.07.012

Roch GJ, Busby ER, and Sherwood NM. 2011. Evolution of GnRH: Diving deeper. *General and Comparative Endocrinology* 171:1-16. https://doi.org/10.1016/j.ygcen.2010.12.014

Roch GJ, Busby ER, and Sherwood NM. 2014. GnRH receptors and peptides: Skating backward. *General and Comparative Endocrinology* 209:118-134. https://doi.org/10.1016/j.ygcen.2014.07.025

Rodríguez D, Bello X, and Gutiérrez-de-Terán H. 2012. Molecular modelling of G protein-coupled receptors through the web. *Molecular Informatics* 31:334-341. 10.1002/minf.201100162

Sali A. 1995. Comparative Protein Modeling by Satisfaction of Spatial Restraints. *Molecular Medicine Today* 1:270-277.

Shen Z, Jiang X, Yan L, Chen Y, Wang W, Shi Y, Shi L, Liu D, and Zhou N. 2018. Structural basis for the interaction of diapause hormone with its receptor in the silkworm, *Bombyx mori*. *The FASEB Journal* 32:1338-1353. 10.1096/fj.201700931R

Siegert K, Morgan P, and Mordue W. 1985. Primary structures of locust adipokinetic hormones II. . *Biol Chem Hoppe-Seyler* 366:723-727.

Sklenar V, Piotto M, Leppik R, and Saudek V. 1993. Gradient-tailored water suppression for 1H-15N HSQC experiments optimized to retain full sensitivity. *J Magn Reson A* 102:241-245.

Stone JV, Mordue W, Batley KE, and Morris HR. 1976. Structure of locust adipokinetic hormone, a neurohormone that regulates lipid utilisation during flight. *Nature* 263:207-211. 10.1038/263207a0

Tieleman DP, Van Der Spoel D, and Berendsen HJC. 2000. Molecular dynamics simulations of dodecylphosphocholine micelles at three different aggregate sizes: Micellar structure and chain relaxation. *Journal of Physical Chemistry B* 104:6380-6388.

596 Tremblay M-L. 2010. The predictive accuracy of secondary chemical shifts is more affected by
597 protein secondary structure than solvent environment. *Journal of Biomolecular NMR* 46:257.
598 10.1007/s10858-010-9400-5

599 Trott O, and Olson AJ. 2010. Software news and update AutoDock Vina: Improving the speed
600 and accuracy of docking with a new scoring function, efficient optimization, and multithreading.
601 *Journal of Computational Chemistry* 31:455-461. 10.1002/jcc.21334

602 Trzaskowski B, Latek D, Yuan S, Ghoshdastider U, Debinski A, and Filipek S. 2012. Action of
603 molecular switches in GPCRs - Theoretical and experimental studies. *Current Medicinal*
604 *Chemistry* 19:1090-1109. 10.2174/092986712799320556

605 Van Der Spoel D, Lindahl E, Hess B, Groenhof G, Mark AE, and Berendsen HJC. 2005.
606 GROMACS: Fast, flexible, and free. *Journal of Computational Chemistry* 26:1701-1718.

607 Veenstra JA. 2014. The contribution of the genomes of a termite and a locust to our
608 understanding of insect neuropeptides and neurohormones. *Front Physiol* 5:454.

609 Verlinden H, Vleugels R, Zels S, Dillen S, Lenaerts C, Crabbé K, Spit J, and Vanden Broeck J.
610 2014. Receptors for neuronal or endocrine signalling molecules as potential targets for the
611 control of insect pests. *Advances in Insect Physiology* 46: 167-303.

612 Vilar S, Ferino G, Phatak SS, Berk B, Cavasotto CN, and Costanzi S. 2011. Docking-based
613 virtual screening for ligands of G protein-coupled receptors: Not only crystal structures but also
614 in silico models. *Journal of Molecular Graphics and Modelling* 29:614-623.
615 10.1016/j.jmgm.2010.11.005

616 Weber PL, Morrison R, and Hare D. 1988. Determining stereo-specific 1H Nuclear magnetic
617 resonance assignments from distance geometry calculations. *J Molec Biol* 204:483-487.

618 Wüthrich K. 1986. *NMR of Proteins and Nucleic Acids*. New York: Wiley.

619 Zubrzycki IZ. 2000. Molecular dynamics study on an adipokinetic hormone peptide in aqueous
620 solution. *Zeitschrift für Naturforschung C, A Journal of Biosciences* 55:125-128.

621

Figure 1(on next page)

Plots of Hα and ^{N}H random coil NMR chemical shift deviations

(a) Schgr-AKH-II (b) Locmi-AKH-I (c) Aedae-AKH. (d) Model-free order parameter, S^2.

PeerJ Preprints | https://doi.org/10.7287/peerj.preprints.27641v1 | CC BY 4.0 Open Access | rec: 8 Apr 2019, publ: 8 Apr 2019

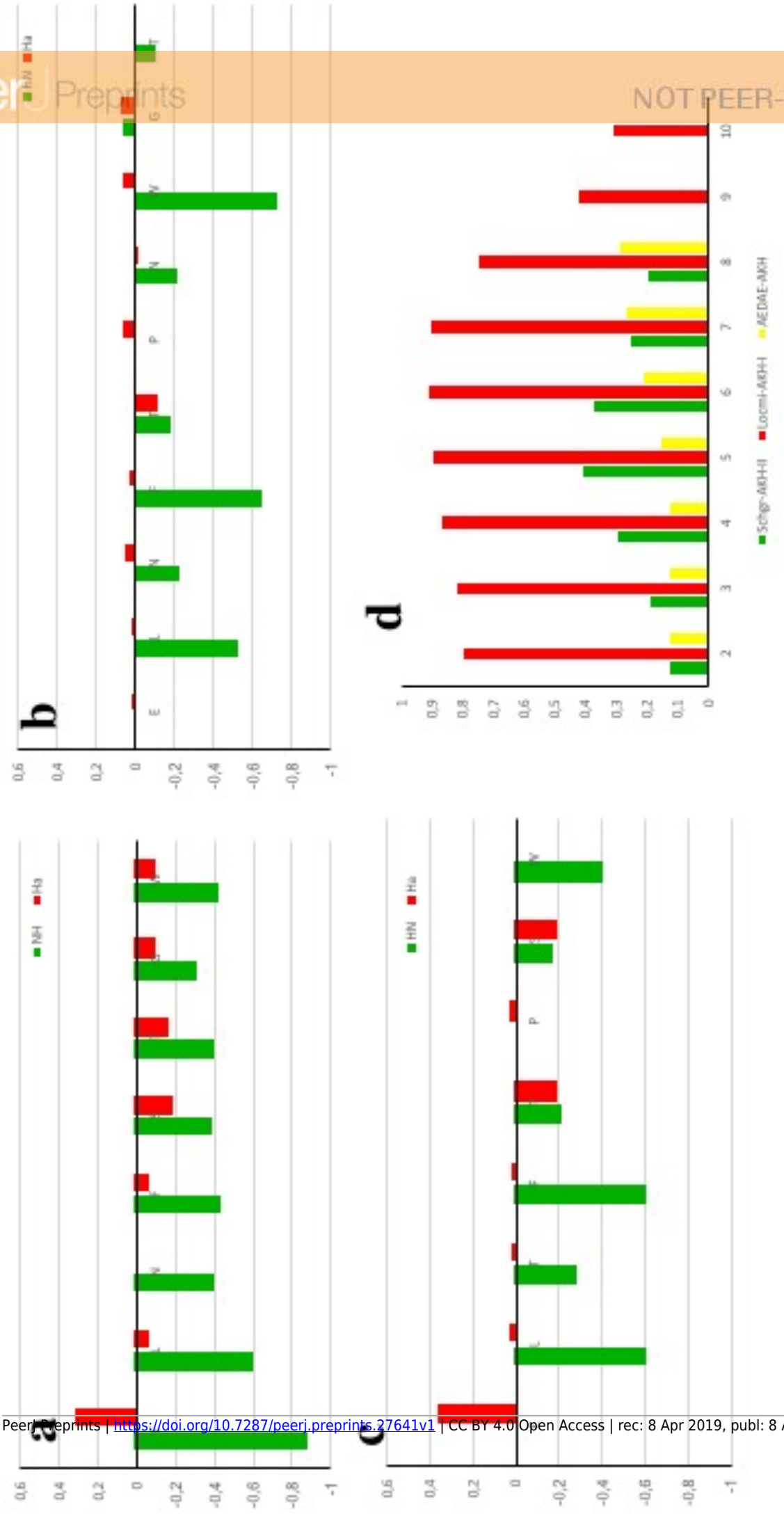

PeerJ Preprints | https://doi.org/10.7287/peerj.preprints.27641v1 | CC BY 4.0 Open Access | rec: 8 Apr 2019, publ: 8 Apr 2019

Figure 2(on next page)

DPC micelle solution cluster overlay and the root conformation for three AKH peptides.

(a) Locmi-AKH-I (b) Aedae-AKH-I and (c) Schgr-AKH-II

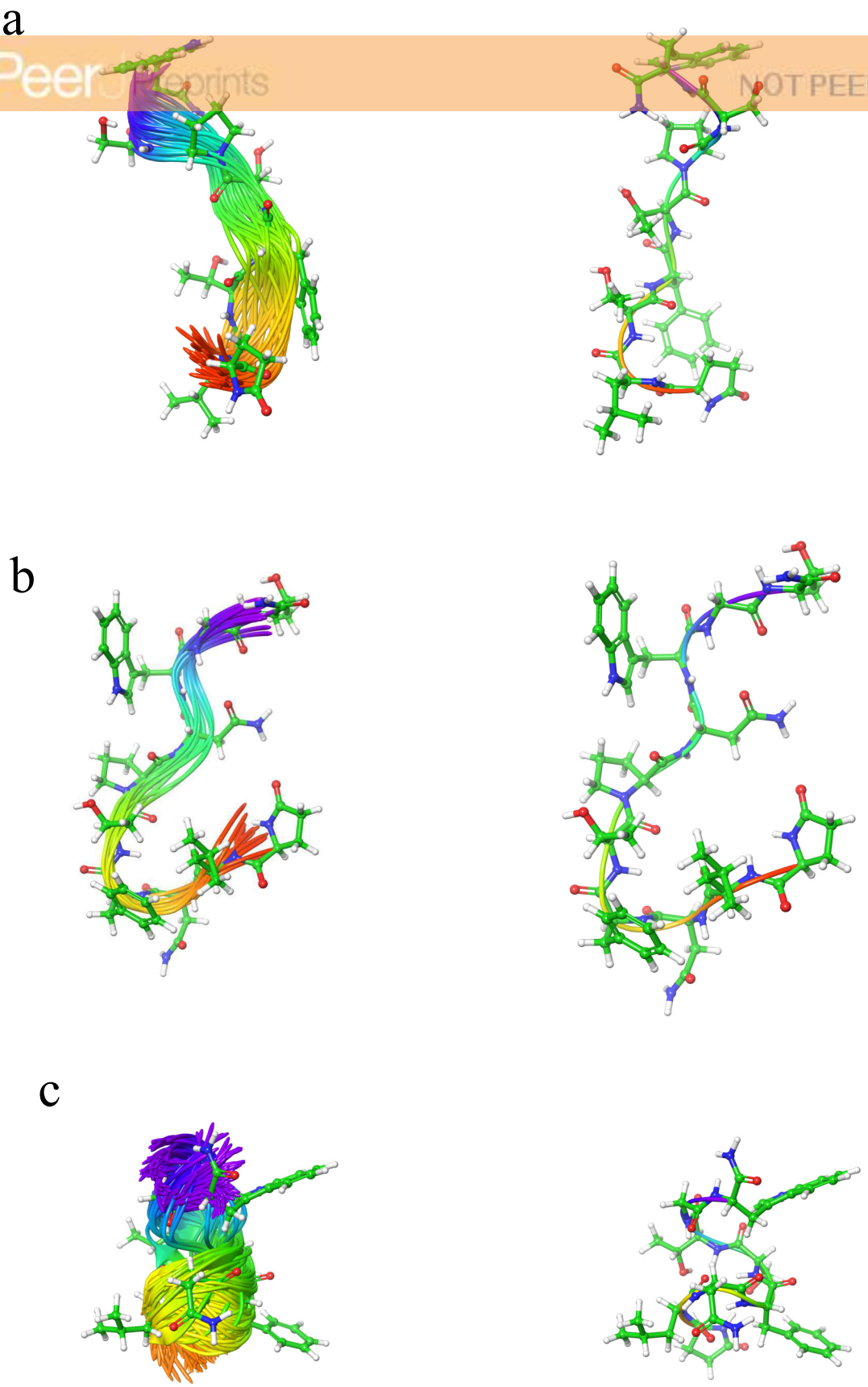

Figure 2 Cluster overlay and single structure for (a) Locmi-AKH-I (b) Aedae-AKH-I and (c) Schgr-AKH-II in DPC micelle solution.

PeerJ Preprints | https://doi.org/10.7287/peerj.preprints.27641v1 | CC BY 4.0 Open Access | rec: 8 Apr 2019, publ: 8 Apr 2019

Figure 3(on next page)

Contact surface area between ligand and DPC micelle as a function of time.

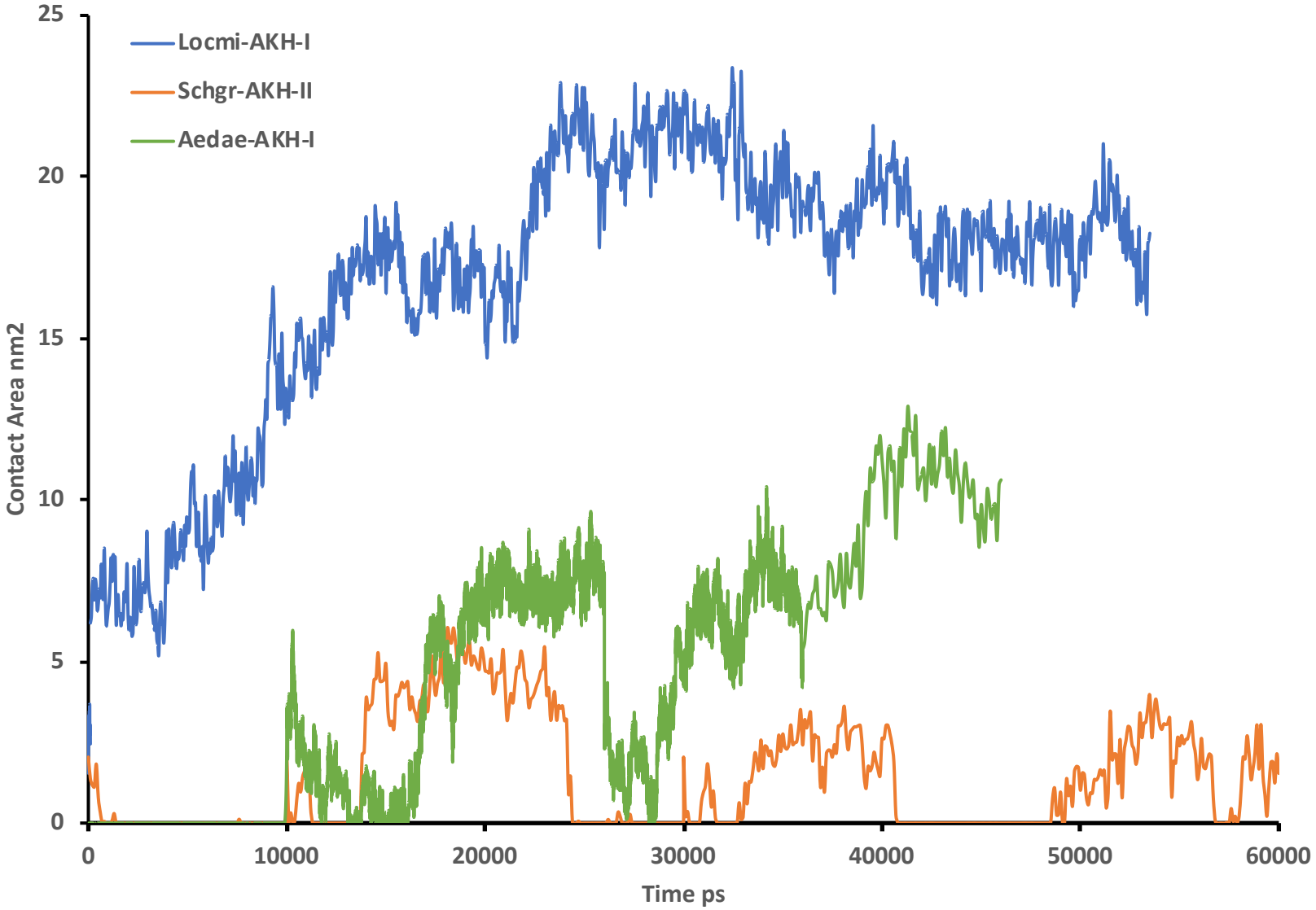

Figure 3. Contact surface area between ligand and DPC micelle as a function of time.

PeerJ Preprints | https://doi.org/10.7287/peerj.preprints.27641v1 | CC BY 4.0 Open Access | rec: 8 Apr 2019, publ: 8 Apr 2019

Figure 4(on next page)

Binding of Schgr-AKH-II to its receptor

(a) Overlay of several snapshots of the dynamic simulation Schgr-AKH-II in its receptor binding pocket, (b) Enlargement of binding pocket showing orientation of peptide, (c) Conformation of best binding pose of Schgr-AKH-II; (d) Overlay of best binding pose and root conformer of DPC simulation.

PeerJ Preprints | https://doi.org/10.7287/peerj.preprints.27641v1 | CC BY 4.0 Open Access | rec: 8 Apr 2019, publ: 8 Apr 2019

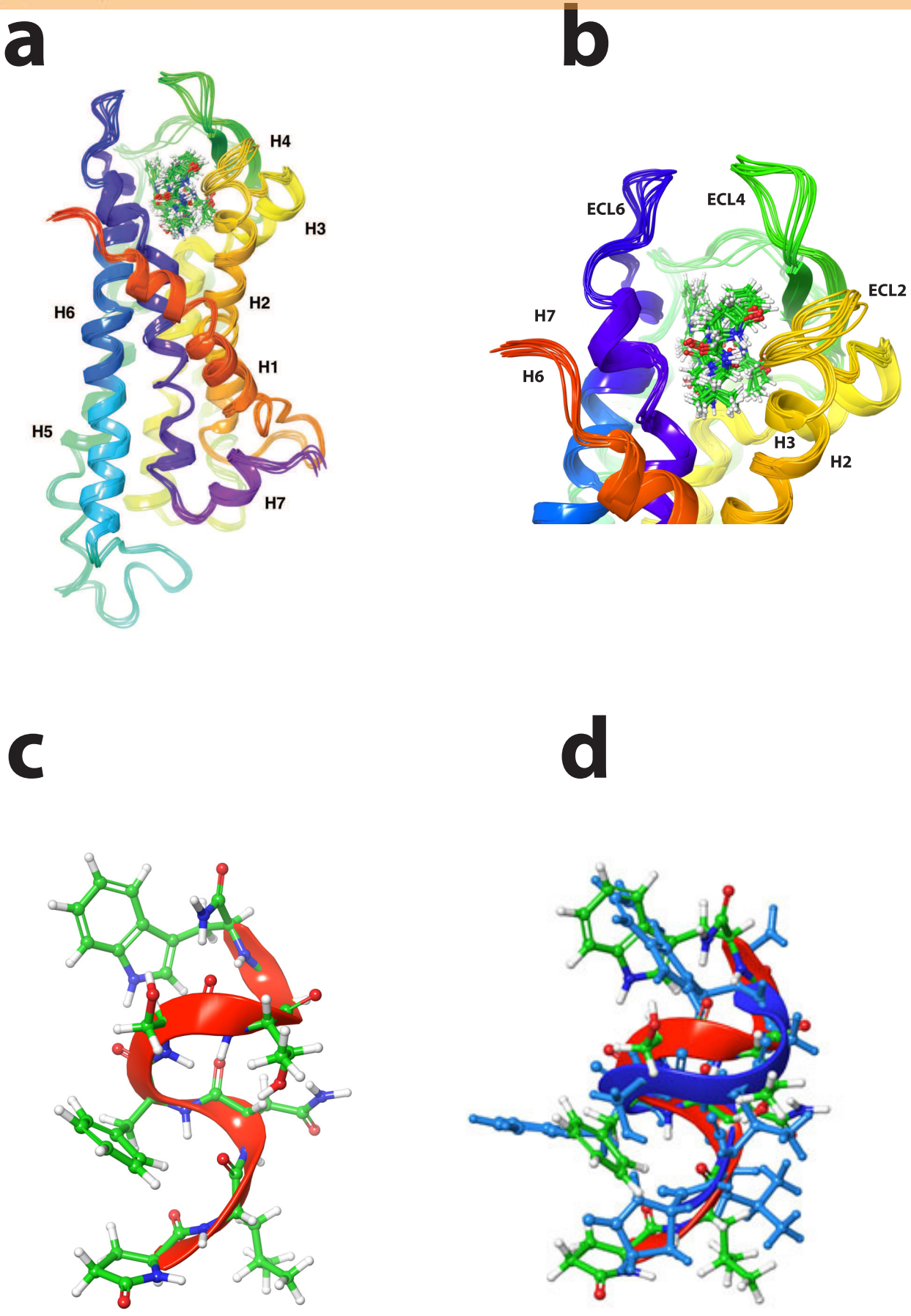
a
H4
H3
H6
H2
H1
H5
H7
b
ECL6
ECL4
ECL2
H7
H6
H3
H2
c
d

Figure 5(on next page)

Binding of Locmi-AKH-I to its receptor

(a) Conformer of Locmi-AKH-I, (b) overlay of Locmi-AKH-I in binding pocket (blue) and in DPC solution, (c) Receptor plus Locmi-AKH-I; (d) Enlargement of binding pocket showing the orientation of the peptide; (e) Binding pocket surface.

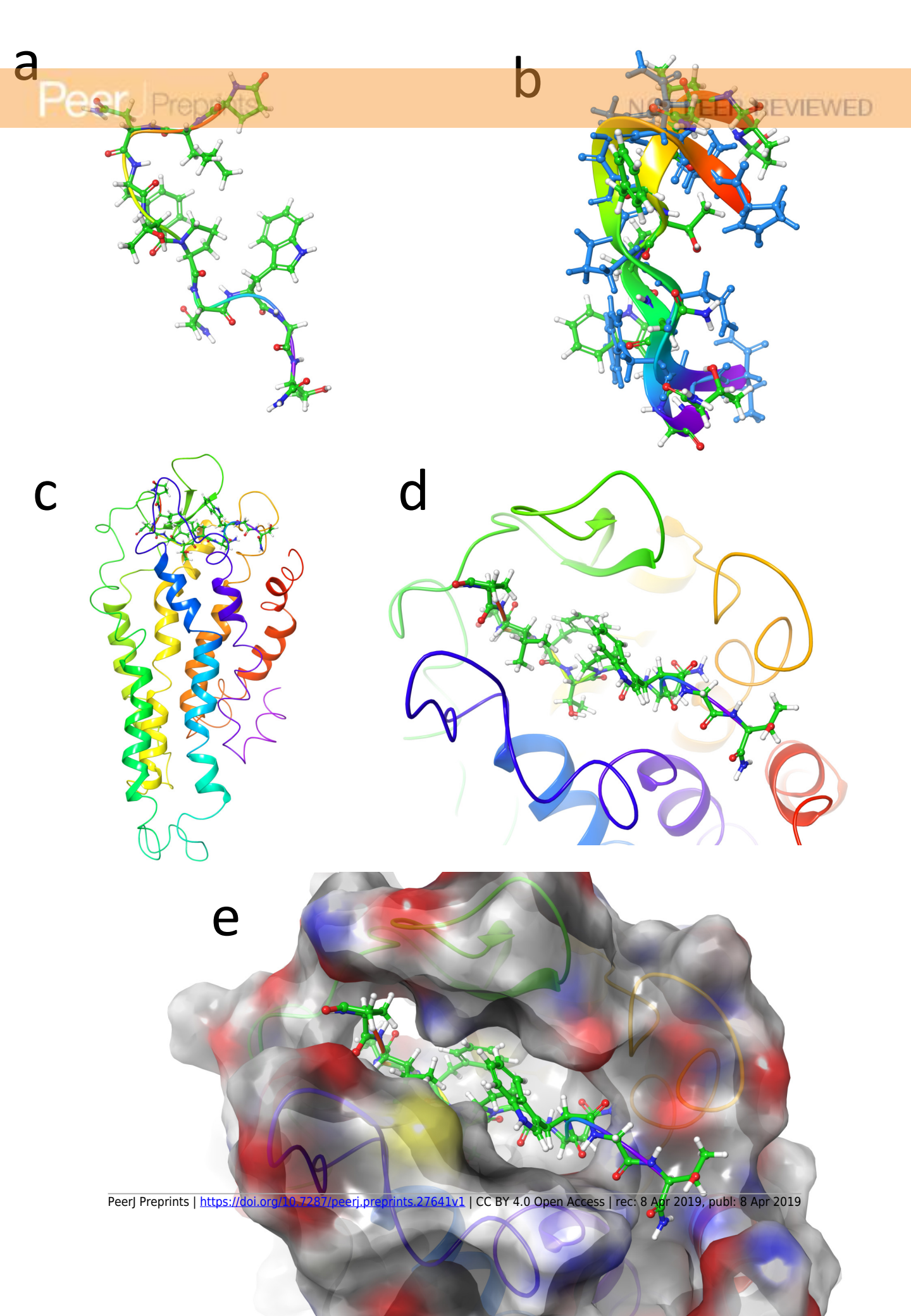

PeerJ Preprints | https://doi.org/10.7287/peerj.preprints.27641v1 | CC BY 4.0 Open Access | rec: 8 Apr 2019, publ: 8 Apr 2019

Figure 6(on next page)

Binding of Aedae-AKH to its receptor

(a) Receptor plus Aedae-AKH (b) Enlargement of binding pocket showing orientation of peptide; (c) Conformer of Aedae-AKH, (d) overlay of Aedae-AKH in binding pocket (blue) and in DPC solution, (e) Binding pocket surface.

PeerJ Preprints | https://doi.org/10.7287/peerj.preprints.27641v1 | CC BY 4.0 Open Access | rec: 8 Apr 2019, publ: 8 Apr 2019

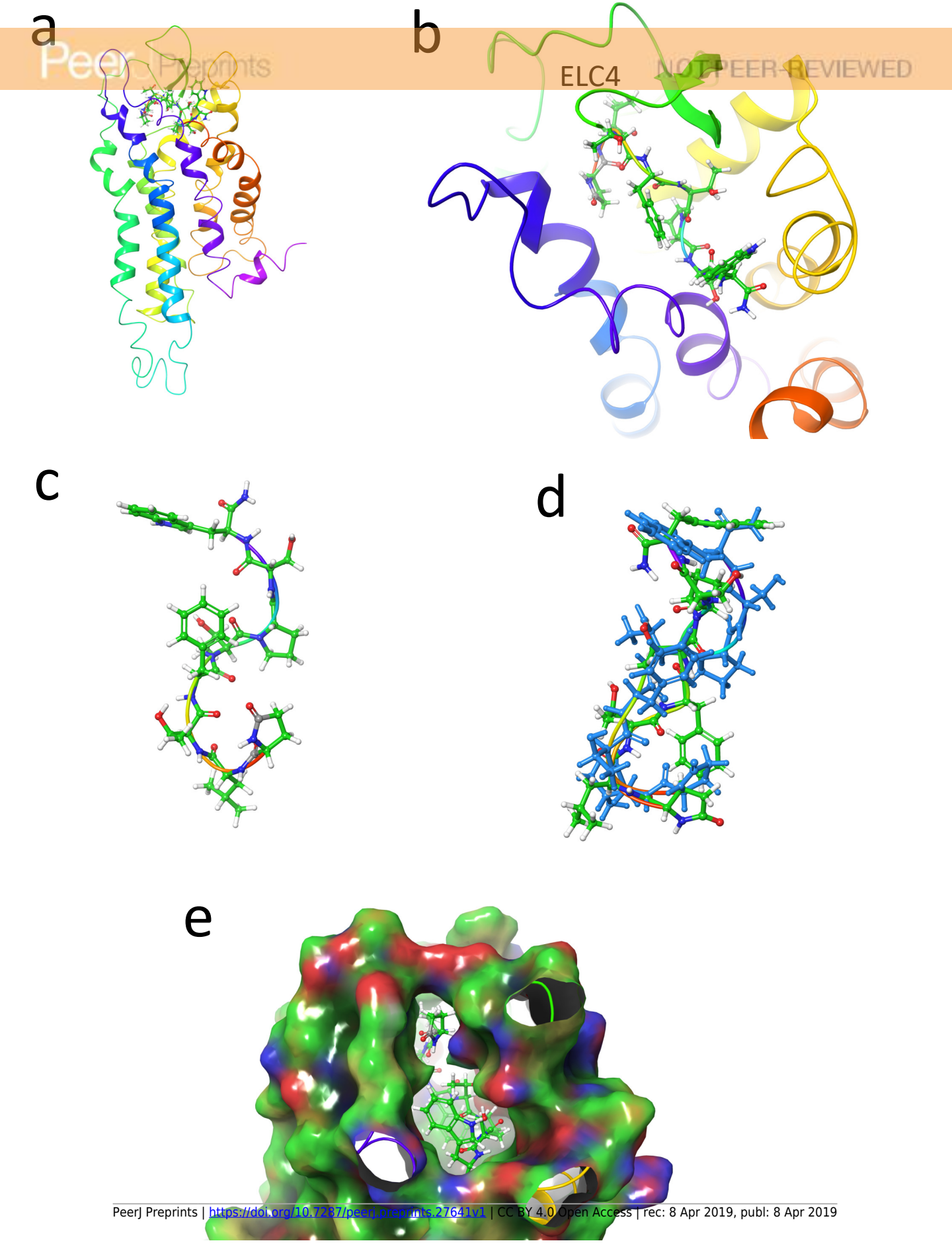

PeerJ Preprints | https://doi.org/10.7287/peerj.preprints.27641v1 | CC BY 4.0 Open Access | rec: 8 Apr 2019, publ: 8 Apr 2019

Figure 7 (on next page)

Ligand interaction diagrams.

(a) Aedae-AKH, (b) Schgr-AKH-II, (c) Locmi-AKH-I

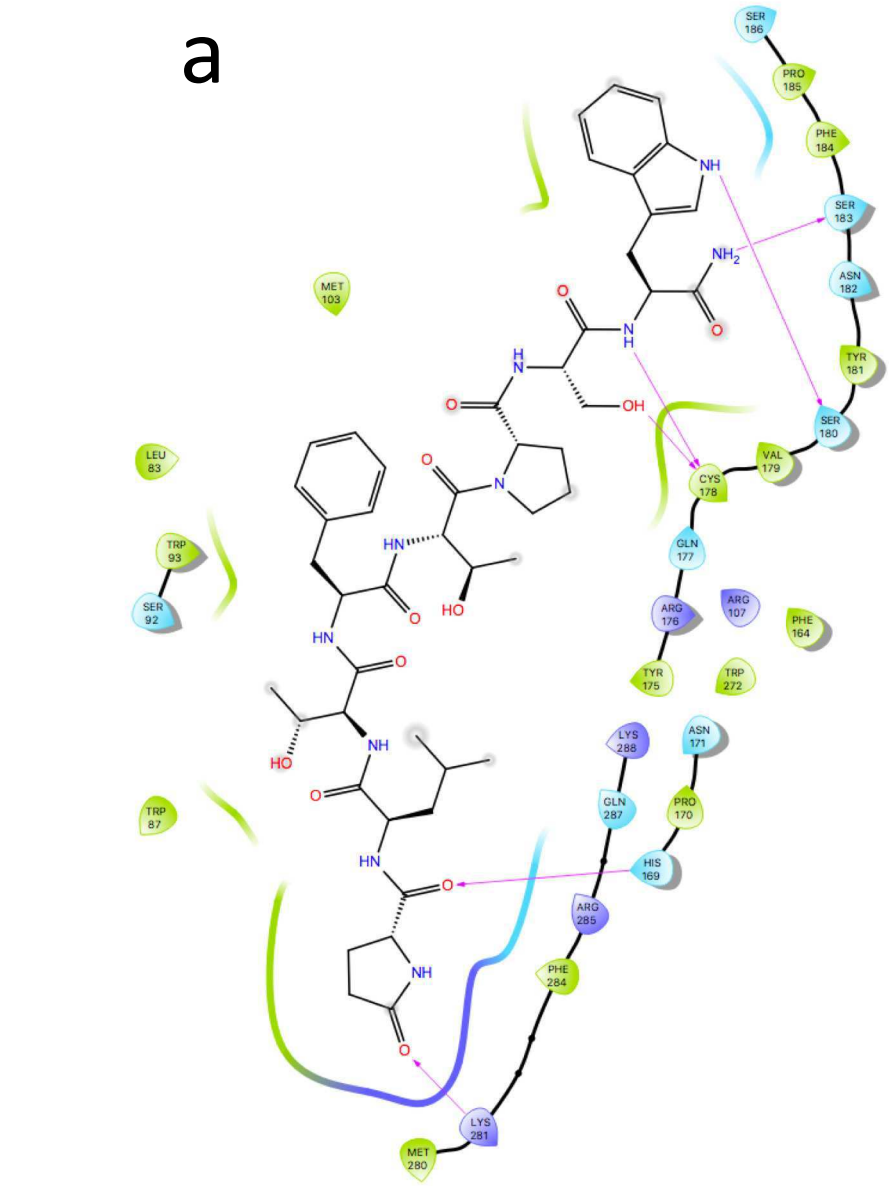

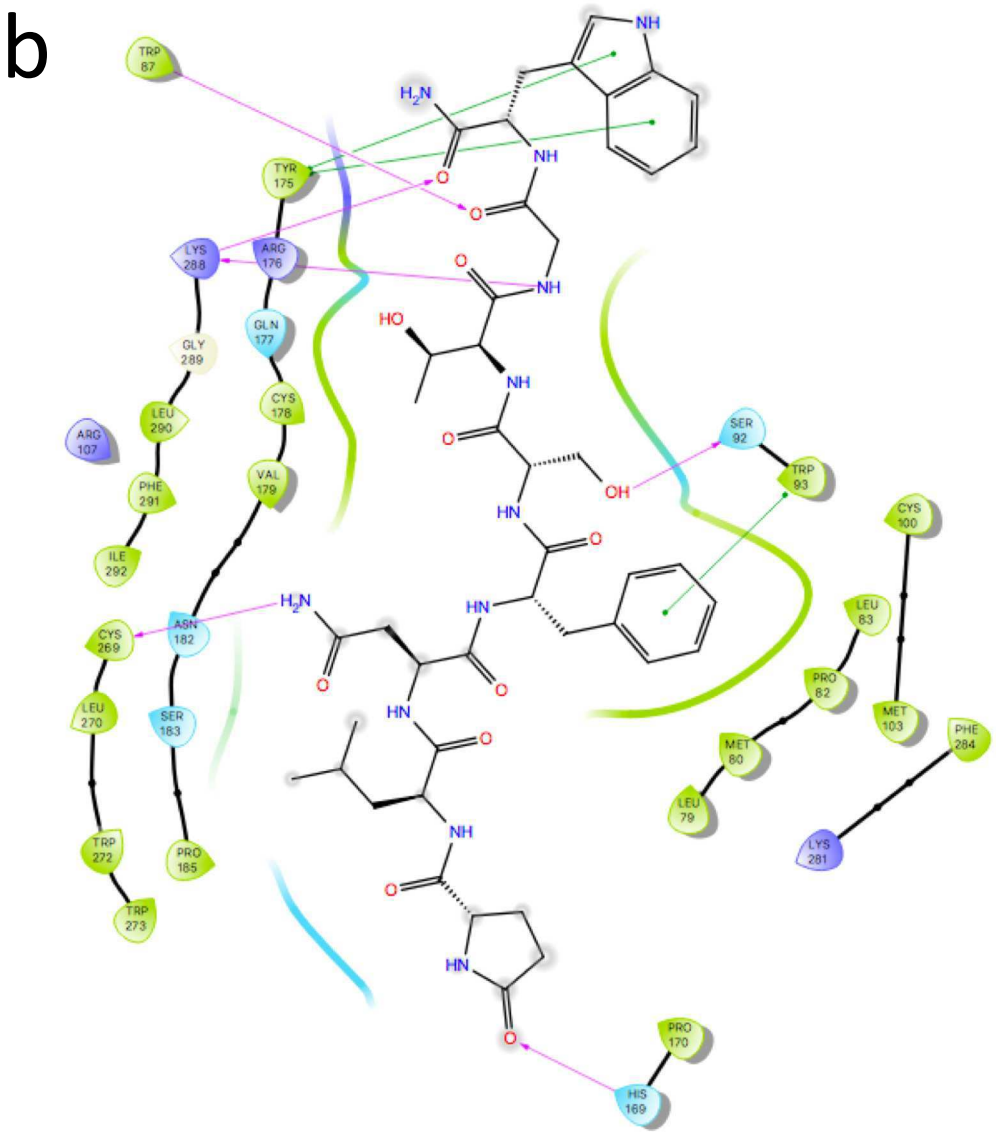

C

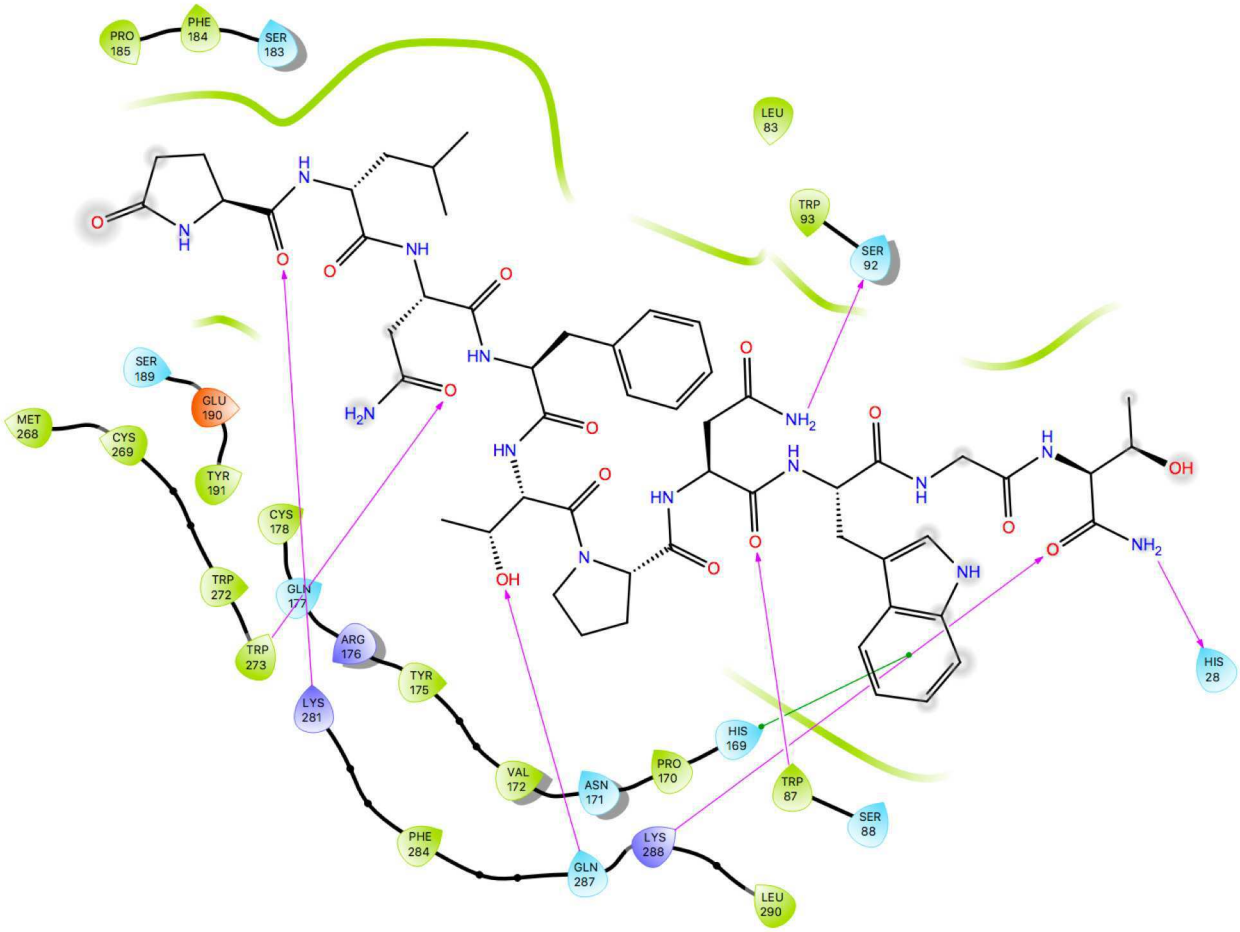

Figure 8(on next page)

Comparison of active and inactive Schgr-AKH-II receptor.

(a) Overlay of active (coloured) and inactive (green) *S. gregaria* receptor (b) Closed DRY switch (c) open DRY switch. Only polar hydrogens are shown.

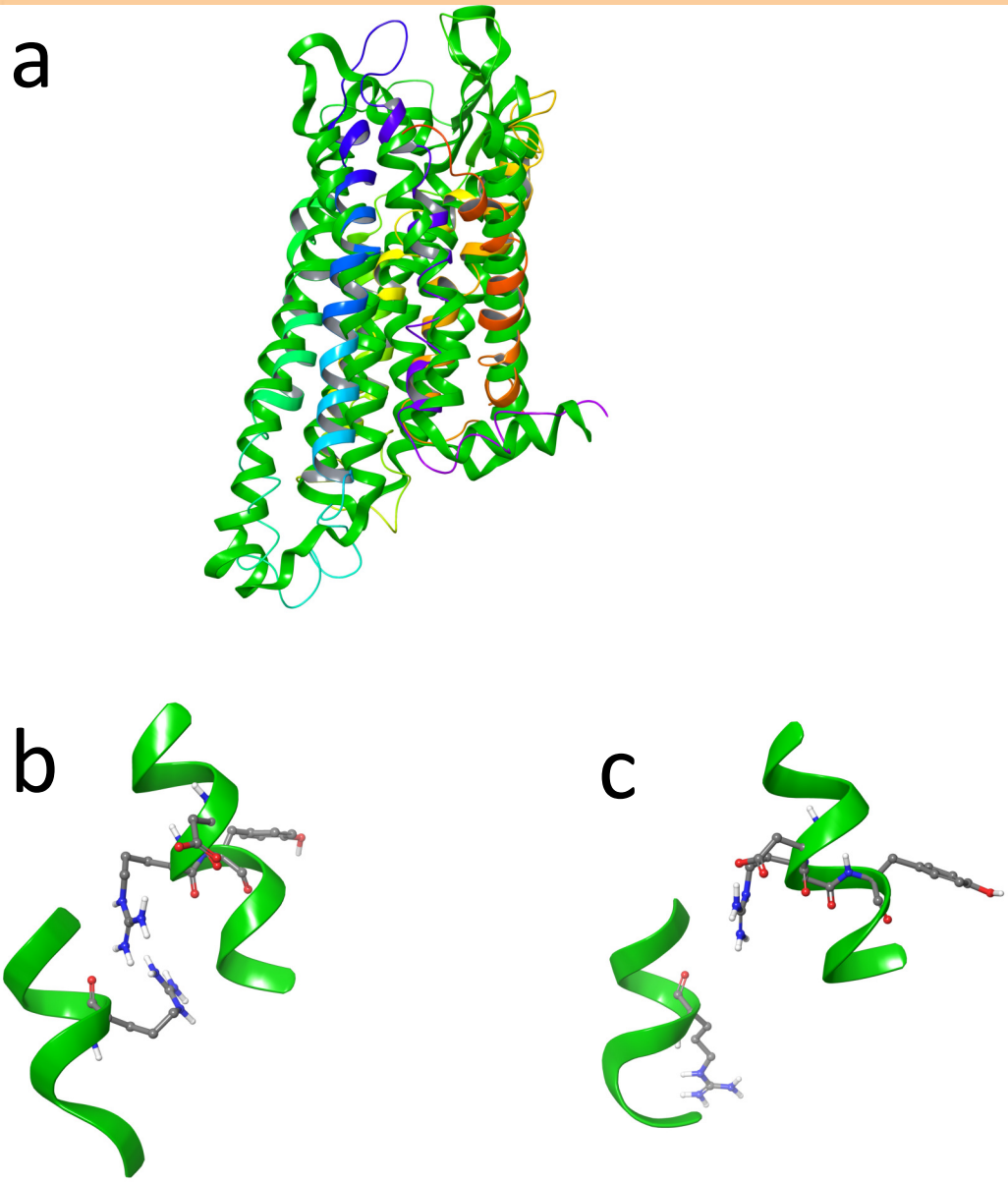

PeerJ Preprints | https://doi.org/10.7287/peerj.preprints.27641v1 | CC BY 4.0 Open Access | rec: 8 Apr 2019, publ: 8 Apr 2019

Figure 9(on next page)

Molecular switches.

(a) TM3-6 lock, active and inactive receptor; (b) Tyrosine toggle switch, active and inactive receptor, (c) CWxPY motif on TM6, active and inactive receptor.

PeerJ Preprints | https://doi.org/10.7287/peerj.preprints.27641v1 | CC BY 4.0 Open Access | rec: 8 Apr 2019, publ: 8 Apr 2019

a

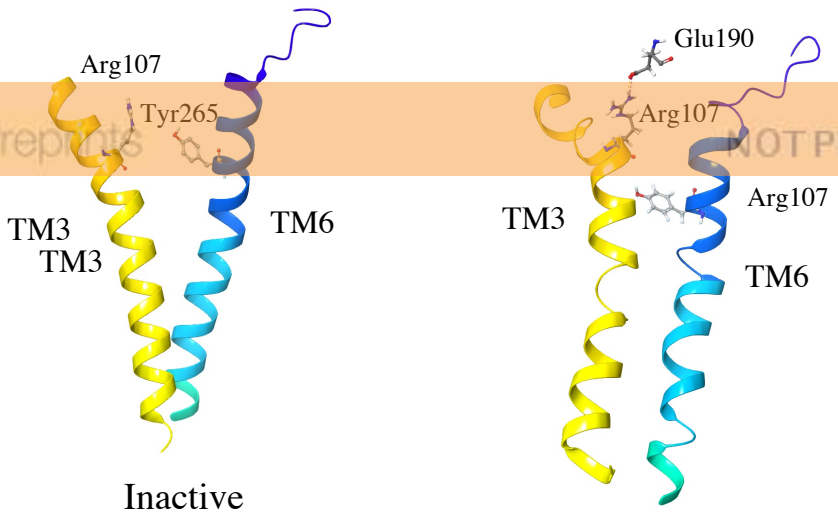

b

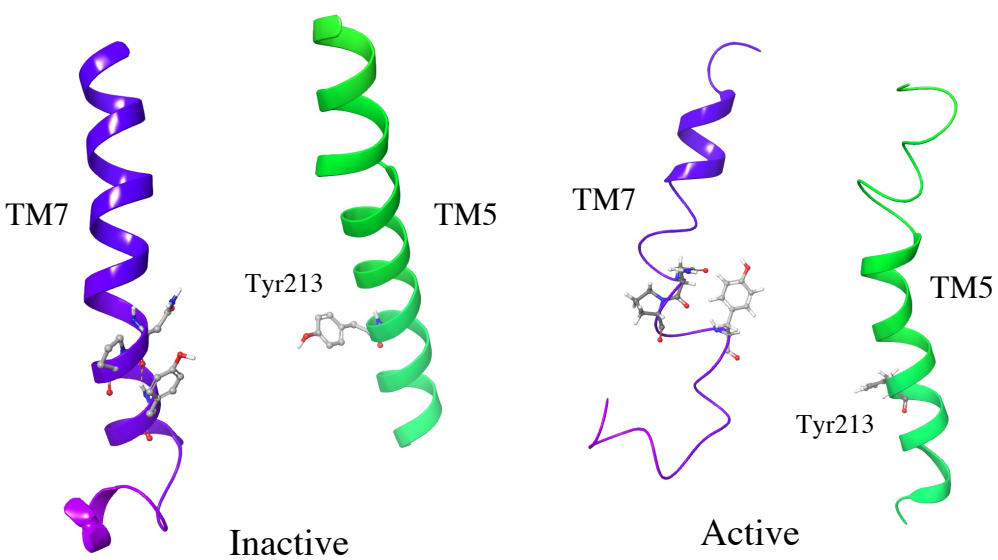

c

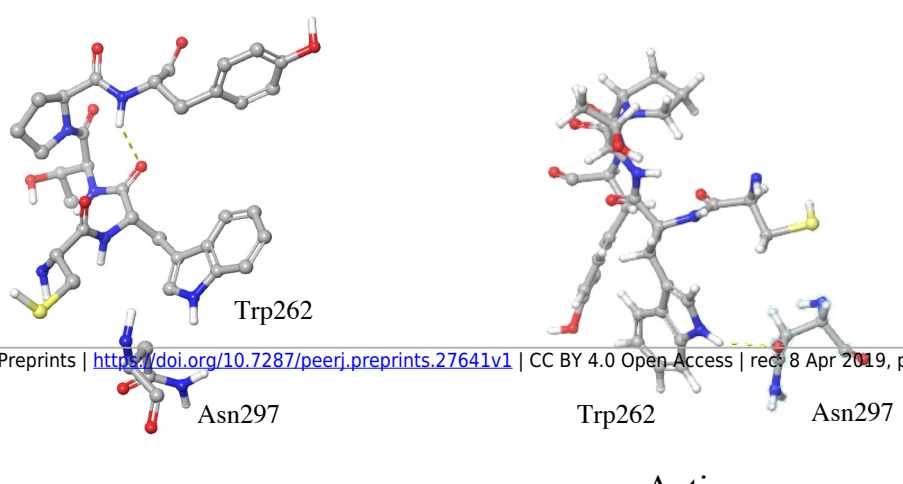

PeerJ Preprints | https://doi.org/10.7287/peerj.preprints.27641v1 | CC BY 4.0 Open Access | rec: 8 Apr 2019, publ: 8 Apr 2019

Table 1(on next page)

Primary structure of the adipokinetic peptides of locusts. Conserved residues are highlighted.

Table 1. Primary structure of the adipokinetic peptides of locusts. Conserved residues are highlighted.

Peptide name	Sequence	Species
Locmi-AKH-I	pELNFTPNWGT amide	*L. migratoria*; *S. gregaria*
Locmi-AKH-II	pELNFSAGW amide	*L. migratoria*
Locmi-AKH-III	pELNFTPWW amide	*L. migratoria*
Locmi-AKH-IV	pELTFTPSW amide	*L. migratoria, S. gregaria*
(= Aedae-AKH)		
Schgr-AKH-II	pELNFSTGW amide	*S. gregaria*

Table 2(on next page)

^{1}H chemical shifts of Schgr-AKH-II: DPC micelle solution, pH 4.5, 20mM phosphate, Temp = 280K.

Table 2. 1H chemical shifts of Schgr-AKH-II:

DPC micelle solution, pH 4.5, 20mM phosphate, Temp = 280K

#	Res	HN	Hα	Hβ (Hβ')	Others
1	Glu	7.742	4.361	2.335,	Hγ:2.483,1.951
2	Leu	8.259	4.232	1.614,1.318	Hδ:0.863
3	Asn	8.364	4.660	2.767,2.647	Hδ:6.864,7.565
4	Phe	7.978	4.561	3.071,2.992	
5	Ser	8.096	4.289	3.782,3.689	
6	Thr	7.923	4.179	3.908	Hγ: 1.040
7	Gly	8.145	3.845,3.905		
8	Trp	7.790	4.587	3.181,3.183	Hδ:7.164,Hε:9.894,7.513,Hζ: 7.360,6.959,Hη:7.005

30% DMSO solution, pH 4.5, 20mM phosphate, Temp = 298 K

#	Res	HN	Hα	Hβ (Hβ')	Others
1	Glu	7.770	4.173	2.238,	Hγ:2.361,1.888
2	Leu	8.199	4.160	1.436,1.304	Hδ:0.732,0.780
3	Asn	8.208	4.501	2.519,2.594	Hδ:6.777,7.440
4	Phe	8.077	4.467	3.046,2.849	
5	Ser	8.134	4.318	3.710,3.667	
6	Thr	7.917	4.165	4.076	Hγ:na,1.050
7	Gly	8.132	3.794,3.691		
8	Trp	7.874	4.466	3.187,3.018	Hδ:7.096,Hε:10.111,7.539,Hζ:7.355,7.021,Hη:7.103

Table 3(on next page)

^{1}H and ^{13}C chemical shifts of Locmi-AKH-I: DPC micelle solution, pH 5.0, 20 mM phosphate, Temp = 285 K.

Table 3 Locmi-AKH-I; pELNTPNWGT-NH2 in DPC solution pH 5.0, Temp = 285K

#	Res	HN	H_α (C_α)	H_β ($H_{\beta'}$) (C_β)	Others
1	Glu		4.09	1.642	Hγ:1.541,1.145
2	Leu	8.271	4.32 (54.7)	1.501,1.715	Hγ:1.620,Hδ:0.978,0.964
				(41.8)	Cδ1 23.4, Cδ2 25.0
3	Asn	8.491	4.71	2.715,2.806	Hδ:6.871,7.585
				(38.6)	
4	Phe	7.768	4.67(52.3)	2.984,3.072	Hδ:7.182,Hε:7.260,Hζ:7.289
				(40.3)	Cδ 131.5, Cε 130.8, Cζ 130.6
5	Thr	7.987	4.49 (57.8)	4.015	Hγ:1.080
				(69.9)	Cγ2 20.7
6	Pro		4.44 (59.0)	2.031,2.586	Hγ:2.418
				(27.8)	Cγ 31.9
7	Asn	8.336	4.68	2.672,2.801	Hδ:6.851,7.563
				(35.6)	
8	Trp	7.529	4.74	3.301	Hδ:7.247, 7.091,Hζ:7.448,7.617,Hη:7.130
				(29.7)	Cδ 126.4, Cε 121.1, Cη 123.6, Cζ 113.5, 120.2
9	Gly	8.316	3.94,4.05 (45.3)		
10	Thr	7.988	4.288 (61.5)		Hγ:1.207 Cγ 21.3

Table 4(on next page)

^{1}H chemical shifts of Aedae-AKH-I: DPC micelle solution, pH 5.0, 20 mM phosphate, Temp = 285K

1 Table 4 Aedae-AKH-I in DPC solution pH 5.0, Temp = 285K

#	Res	HN	HA	HB (HB')	Others
1	Glu		4.41	2.36	Hγ:2.53, 1.962
2	Leu	8.26	4.38	1.47, 1.66	Hγ:1.68, Hδ:0.91, 0.932
3	Thr	8.20	4.33	4.18	Hγ:1.10
4	Phe	7.82	4.66	3.28	Hδ:7.15, Hε:7.22, HZ:7.25
5	Thr	7.96	4.42	3.93	Hγ:1.02
6	Pro		4.42	1.44, 1.56	Hγ:1.97, 2.53, Hδ:3.08, 3.38
7	Ser	8.28	4.25	3.81	
8	Trp	7.82	4.63	2.93, 3.04	Hδ:7.21, Hε:9.99, 7.06, Hζ:7.40, 7.58, Hη:7.09

2

3

Table 5(on next page)

List of interactions of ligand/receptor in binding pocket of Schgr-AKHR receptor.

PeerJ Preprints | https://doi.org/10.7287/peerj.preprints.27641v1 | CC BY 4.0 Open Access | rec: 8 Apr 2019, publ: 8 Apr 2019

Table 5. List of interactions of ligand/receptor in binding pocket of Schgr-AKHR receptor.

Schgr_AKH		Locmi-AKH		Aedae-AKH	
Ligand	Receptor	Ligand	Receptor	Ligand	Receptor
$pE^{1}O_{\varepsilon 1}$	His169	$pE^{1}CO$	Lys281	$pE^{1}CO$	His169
$N^{3}NH_{2}$	Cys269	$N^{3}CO$	Trp273	$pE^{1}O_{\varepsilon 1}$	Lys281
$F^{4}\pi$-π stack	Trp93	$T^{5}OH$	Gln287	$S^{7}OH$	Cys178
$S^{5}OH$	Ser92	$N^{7}CO$	Trp87	$S^{7}NH$	Cys178
$G^{7}NH$	Lys288	$N^{7}NH_{2}$	Ser92	W^{8} $H_{\varepsilon 1}$	Ser180
$G^{7}CO$	Trp87	$T^{10}CO$	Lys288	$W^{8}NH_{2}$	Ser183
$W^{8}CO$	Lys288	W^{8} π-π stack	His169		
$W^{8}\pi$-π stack	Tyr175	$T^{10}NH_{2}$	His28		